21, rue d'Artois, F-75008 PARIS
http : //www.cigre.org

CIGRE US National Committee
2023 Grid of the Future Symposium

Analysis of Unexpected Line Distance Protection Operation Caused by Islanded Hydro Generation Unit

T. LIN*, K. A. ZAFAR, M. J. TILL
Dominion Energy
USA

SUMMARY

A trip and instantaneous reclose operation on a 230kV transmission line owned by Dominion Energy bypassed the sync check function on a hydro generation unit. This resulted in the unit operating in an islanding condition for 26 cycles before it reconnected to the grid, 133 degrees out-of-sync. As a result, an unfaulted line between the unit and the grid tripped on its Zone 1 protection.

This paper investigates how the islanding condition was generated and examines the data collected from digital fault recorders (DFRs) and protective relays to determine the cause of misoperation at the unfaulted line. High-resolution DFR data allows for detailed observation of the generator's out-of-sync condition and grid reconnection. Plotting the impedance trajectory through the distance protection relay zones during the event provides additional insights into relay operation.

The paper also discusses the concept of Mho distance protection and how its performance is affected during a power swing.

KEYWORDS

Power swing, Out-of-sync, Source Impedance Ratio, Mho Distance Protection, Positive Sequence Voltage Polarization, Islanding

Te-Yu.Lin@dominionenergy.com

1. INTRODUCTION

On May 25th, 2022, a 230 kV transmission line experienced a lightning strike; the line breakers at both ends tripped and reclosed instantaneously. A simplified one-line diagram of this is shown in Fig. 1. Since two nearby network lines were out of service for planned work at the time, a hydro-powered generator was on a radial feed out of the grid. Consequently, when Line F tripped, the generator no longer had a load and accelerated for 26 cycles. When Line F instantaneously reclosed, the generator was reconnected 133 degrees out-of-step with the rest of the system. This out-of-step reclose caused Relay 1 at Line B to trip on Zone 1 protection. The generator's output oscillated, and it eventually tripped on loss of excitation protection after 5.36 seconds. Finally, Relay 1 reclosed after 20 seconds and remained in service.

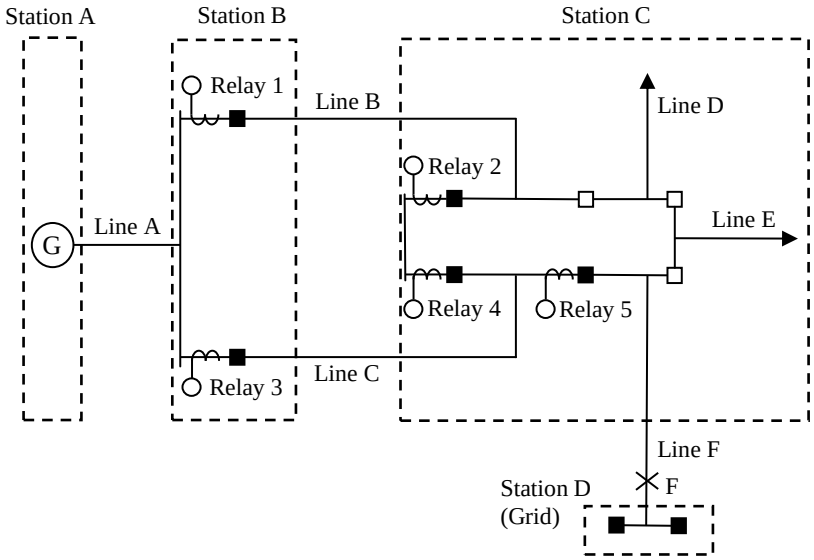

Fig. 1. Simplified one-line diagram of the system

Immediately following the line operation, an investigation began to determine the location of the fault. The system operations team presented several observations to the event analysis group but, due to the lack of high precision time data in the SCADA system, they could not guarantee accurate sequencing of events. The system operators noted that Line F had tripped and reclosed, and the Station B Line B terminal breaker had also tripped and reclosed. The single 55 MW generator also tripped offline; however, it was not known what initiated the trip. Using automated lightning detection and geolocation tools, the event analysis team was able to discern that the initial fault had occurred due to a lightning strike on the Line F C-phase conductor.

Next, focus was directed towards the Station B Line B breaker. While collecting the records from Relay 1, the team was able to view DFR records from the grid-synchronized and generator-islanded portions of the system. Due to the availability of these high-precision time synchronized records, the team was able to create a simplified timeline of events, which is shown in Fig. 2.

The following questions were raised during the event investigation.

- Why did Relay 1 trip?
- If Relay 1 operated correctly, why didn’t Relay 2 trip?
- As Line C and Line B are parallel line systems, why didn’t Relay 3 trip in the same manner as Relay 1?
- What relays should be able to identify and trip on the occurrence of the out-of-sync connection event?
- Why did Relay 5 instantaneously reclose?

In the following sections, we explore the concept of distance protection and its apparent impedance, as seen by the relay during oscillation, to gain a better understanding of how an out-of-step connection can lead to misoperation of distance relay protection.

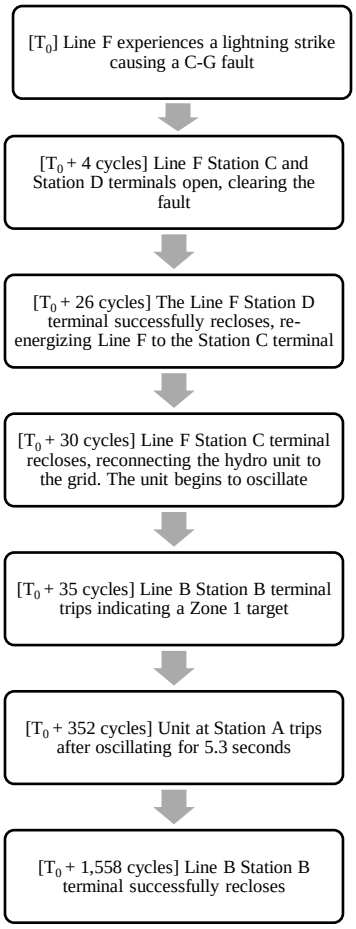

Fig. 2. Relative timeline of events where T0 is the time of the initial fault

2. MHO DISTANCE PROTECTION

Distance protection is widely used for transmission lines. It offers high-speed tripping for up to 80% of the line, which allows for simpler coordination than overcurrent protection. In distance protection, the distance relay measures the impedance of a line and compares it to a set impedance percentage. In the event of a fault, the measured impedance decreases due to the high fault current and low fault voltage. If the measured impedance is lower than the set value, then the fault is identified as being within the protection zone, prompting the circuit breaker to trip. We used the three-phase calculation in the subsequent subsections to provide clarity and simplify the explanation. This paper aims to provide an overview of distance protection theory, rather than focus on how microprocessor relays implement the design [2]. Therefore, the phase angle relationship (ZI-V) was not used in this paper.

2.1. SELF-POLARIZATION

One option when calculating impedance is to use the measured voltage and current on the faulted phase. This method is known as self-polarization [1].

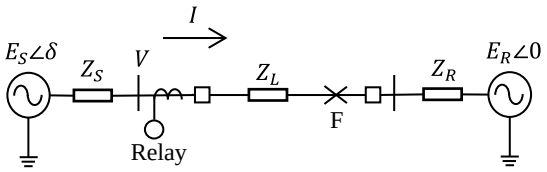

Fig. 3. Two machine system

To draw the Mho circle for the system shown in Fig. 3, we placed a three-phase fault at each point from the relay location to the reach set point of the zone protection setting; we then calculated the impedance Z_r by using faulted voltage and current, as shown in equation (1).

$$Z_r = \frac{V}{I} \tag{1}$$

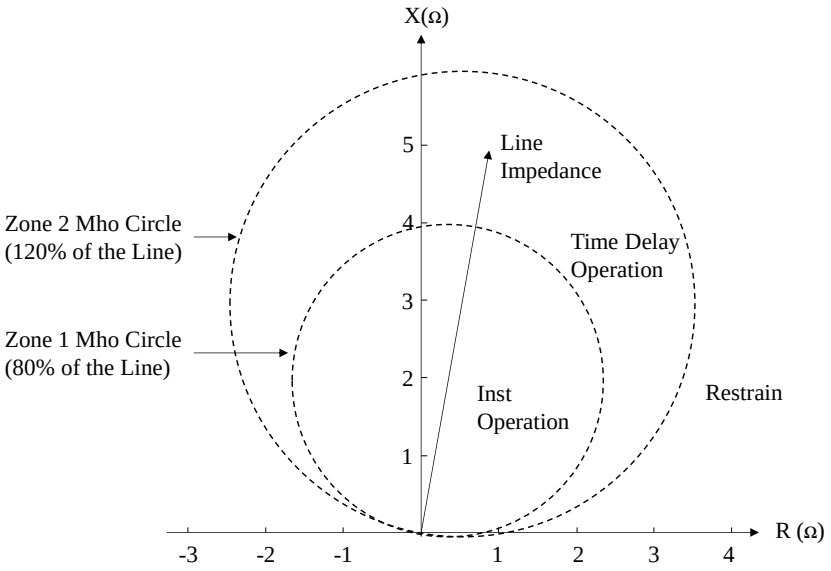

Fig. 4. Self-polarized Mho circle

As Fig. 4 shows, if the apparent impedance Z_r is smaller than the settings of the reaching zone, the point will be within the Mho circles, which could indicate a potential fault on the transmission line. For example, if the point falls within the locus of Zone 1, the relay should issue an instantaneous trip signal to clear the fault.

However, the performance of the self-polarized Mho distance method is reduced when it operates on close-in faults because the faulted phase voltage is too small to provide an accurate impedance calculation [1]. To improve the reliability of the relay, we introduced cross-polarization.

2.2. CROSS-POLARIZATION

This strategy utilized the unfaulted voltage in the calculation to reduce the effect of the inaccurately measured voltage. Positive sequence voltage is often used, as it takes into account all three phases. Equation (2) shows the Mho circle impedance calculated using positive sequence voltage.

$$Z_{r1} = \frac{V_1}{I} \tag{2}$$

However, positive sequence voltage still has limitations when operating for three-phase close-in faults. To remedy this, we used a memory filter to allow the voltage to decline gradually over several cycles, thereby mitigating the effect of inaccurate voltage.

2.3. POSITIVE SEQUENCE MEMORY POLARIZATION

The modern microprocessor relay offers several benefits, including easy implementation of the memory filter and the flexibility to select the length of the memory time for the Mho calculation. The memorized pre-fault voltage can be used to calculate the Mho circle impedance, as demonstrated in equation (3). This results in the Mho circle expanding, allowing for improved fault coverage compared to the self-polarized circle.

$$Z_{r1mem} = \frac{V_{1\,mem}}{I} \tag{3}$$

At the start of a fault occurrence, the $V_{1\,mem}$ is equal to the E_S, as shown in (4). Therefore, when the voltage is divided by the fault current, the Mho impedance Z_{r1mem} can be calculated as the sum of the source impedance Z_{S1} and the impedance seen by the relay to the reach set point Z_r, as shown in (5).

$$Z_{r1mem} = \frac{E_S}{I} \tag{4}$$

$$Z_{r1mem} = Z_{S1} + Z_{r1} \tag{5}$$

As a result, the Mho circle is expanded. However, due to the gradual decline of the memory voltage towards the faulted voltage, the expanded Mho circle will eventually shrink to the same area as the self-polarized circle. The expansion ratio is relative to the source impedance ratio (SIR).

$$SIR = \frac{Z_{S1}}{Z_{r1}} \tag{6}$$

According to IEEE C37.113 - IEEE Guide for Protective Relay Applications to Transmission Lines [3], long transmission lines are classified as having a SIR of less than 0.5, while short transmission lines have a SIR of greater than 4. In Fig. 5, we plotted the expanded Mho circle at SIR equals 0.5, 2, and 4, respectively, to better understand the discrepancy in fault coverage between long and short transmission lines.

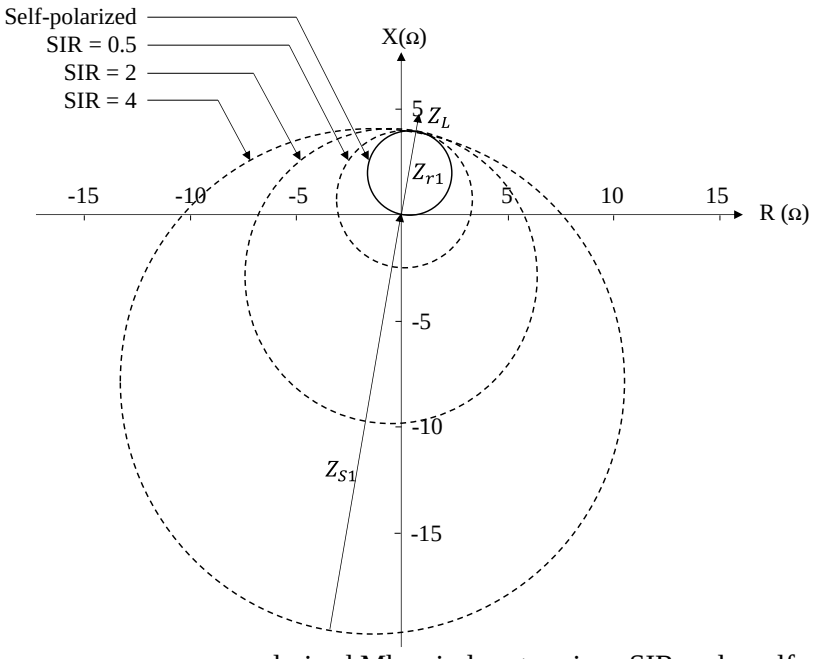

Fig. 5. Positive-sequence memory polarized Mho circles at various SIR and a self-polarized Mho circle

Fig. 5 demonstrates a direct correlation between SIR and the size of the expanded Mho circle; the greater the SIR (the shorter the transmission line), the larger the Mho circle. While this expansion improves fault coverage during a three-phase close-in fault, it could compromise the reliability of Mho distance protection during power swings, especially for a short transmission line.

3. APPARENT IMPEDANCE SEEN BY DISTANCE RELAY DURING POWER SWING

The impact of a power swing on the apparent impedance seen by the distance relays at both ends of the line may lead to the relay's misoperation. The two-machine system illustrated in Fig. 6 is an idealized model used to analyze distance relays' performance during power swings. Shown are the internal voltages of the source $E_S\angle\delta$ and receiving end $E_R\angle 0$, the source and receiving end's impedance $Z_S, Z_R,$, and line impedance Z_L. The phase angle of the receiving end source is used as a reference, and δ represents the voltage angle difference between the two sources.

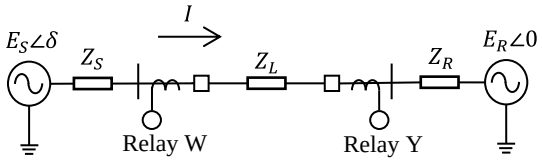

Fig. 6. Two machine system with distance relays

The current measured by the Relay W is given in equation (7), and the measured voltage is in equation (8).

$$\bar{I}_W = \frac{E_S\angle\delta - E_R\angle 0}{Z_S + Z_L + Z_R} \tag{7}$$

$$\bar{V}_W = E_S\angle\delta - Z_S \cdot \overline{\bar{I}_W} \tag{8}$$

Hence, the apparent impedance $\bar{Z}_W$ seen by the Relay W is

$$\bar{Z}_W = \frac{\bar{V}_W}{\bar{I}_W} = (Z_S + Z_L + Z_R)\frac{1}{1 - \left(\left|\frac{E_R}{E_S}\right|\angle -\delta\right)} - Z_S \tag{9}$$

By applying the same methodology, we can determine the apparent impedance $\bar{Z}_Y$ seen by Relay Y, as expressed in equation (10).

$$\bar{Z}_Y = (Z_S + Z_L + Z_R)\frac{1}{1 - \left(\left|\frac{E_S}{E_R}\right|\angle\delta\right)} - Z_R \tag{10}$$

Using equations (9) and (10), we plotted the impedance trajectories in the R-X plane. We also plotted the Zone 1 protection Mho circle using self-polarized and positive sequence polarized elements, as shown in Fig. 7. From the diagram, we can draw four conclusions:

1. When the system angle difference δ was between 110 and 250 degrees (the value varied depending on the system condition), the impedance trajectory of Relay W entered the expanded Mho Zone 1 protection, even though there was no fault on the transmission line.
2. The impedance trajectory of Relay Y was similar to Relay W but reversed, as the current flowed in the opposite current direction. This indicated that Relay Y did not respond to the same power swing angle as Relay W. It appeared that the behavior of the distance relays at both ends was not consistent during the power swing. The same conclusion could also be applied to multi-machine systems [4].

3. The self-polarized Mho element was a static circle that remained constant regardless of the fault current direction, load flow, or source impedance [5].
4. The positive-sequence polarized Mho was dynamic and could vary with the fault current direction, the load flow, or SIR [5]. If the SIR was low, the Mho circle was less expanded than when the SIR was high. This indicated that the relay was less likely to misoperate and more aligned with the self-polarized Mho circle.

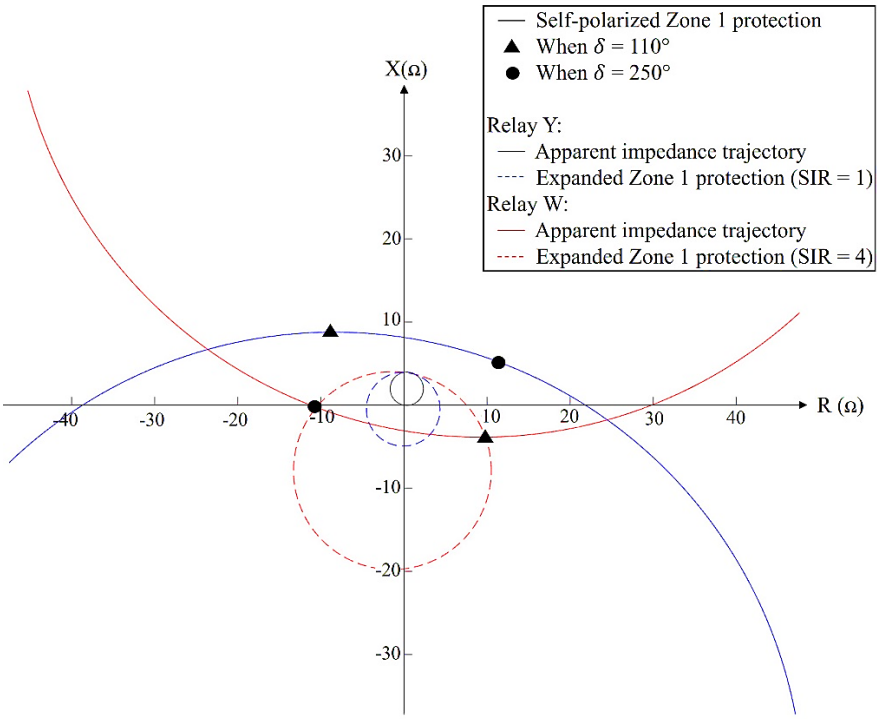

Fig. 7. The trajectory of apparent impedances seen by distance relays at both ends during power swings

4. EVENT ANALYSIS

The operational review of the event involved analyzing each relay's behavior and answering questions that arose during the investigation. Tables I and II summarize the local system parameters and relevant relay settings.

Table I. Relay Settings

Relay ID	Source Impedance Ratio (SIR)	Zone 1 Reach	Zone 2 Reach	Reclosing (seconds)
Relay 1	28.97	80%	150%	25
Relay 2	3.00	80%	150%	INST, 15, 80
Relay 3	29.59	OFF	150%	20
Relay 4	2.99	80%	150%	INST, 15, 75
Relay 5	1.18	80%	150%	INST, 15, 75

Table II. Line Data

Line #	Length (miles)	Voltage (kV)	Impedance (Ω, sec)	
			Positive	Zero
Line A	0.13	230	0.05∠81.11	0.07∠75.57
Line B	8.69	230	1.32∠83.05	3.89∠71.38
Line C	8.62	230	1.32∠83.05	3.79∠71.93
Line F	16.43	230	2.59∠81.44	5.44∠73.06

Fig. 8 indicates an angle divergence of 133 degrees between the grid and the islanded hydro generation unit, prior to reconnection. The significant angle difference suggests that the impedance trajectory was close to the Mho protection circle. This information is crucial for the following analysis.

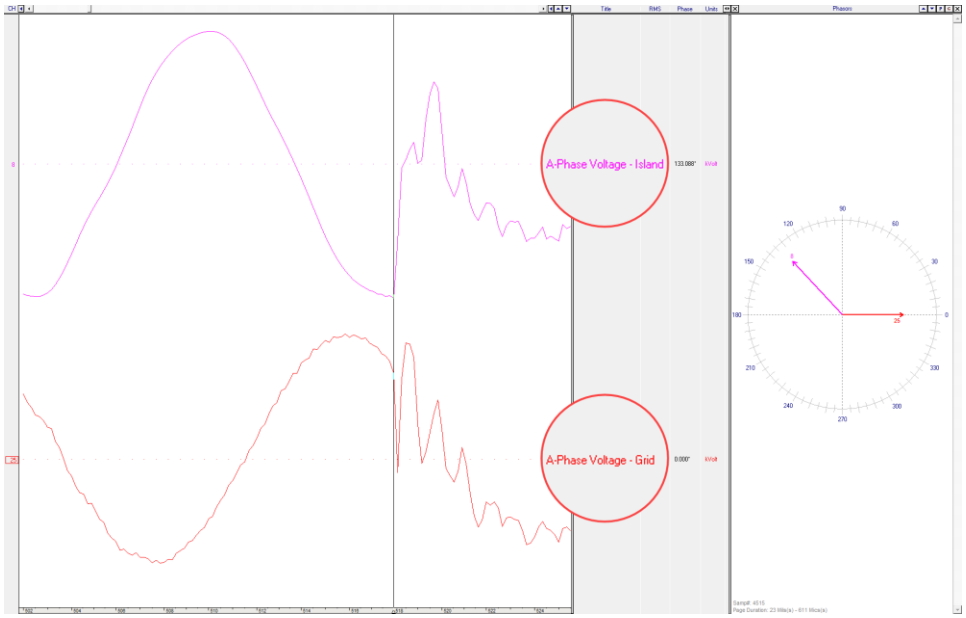

Fig. 8. Phase angle deviation at time of breaker closing and synchronizing island with grid

4.1. RELAY 1 ANALYSIS

According to the relay manual, Relay 1 uses positive-sequence memory voltage as the polarizing quantity for distance element calculations. Therefore, we needed to take into account the Mho circle expansion chracteristic when analyzing the relay's performance during the event. In Fig. 9, the impedance trajectory of the A-B phase element (ZAB) did not enter the self-polarized Mho circle. However, due to the high SIR, the Mho circle expanded, allowing the impedance trajectory to enter the expanded circle, causing Relay 1 to misoperate.

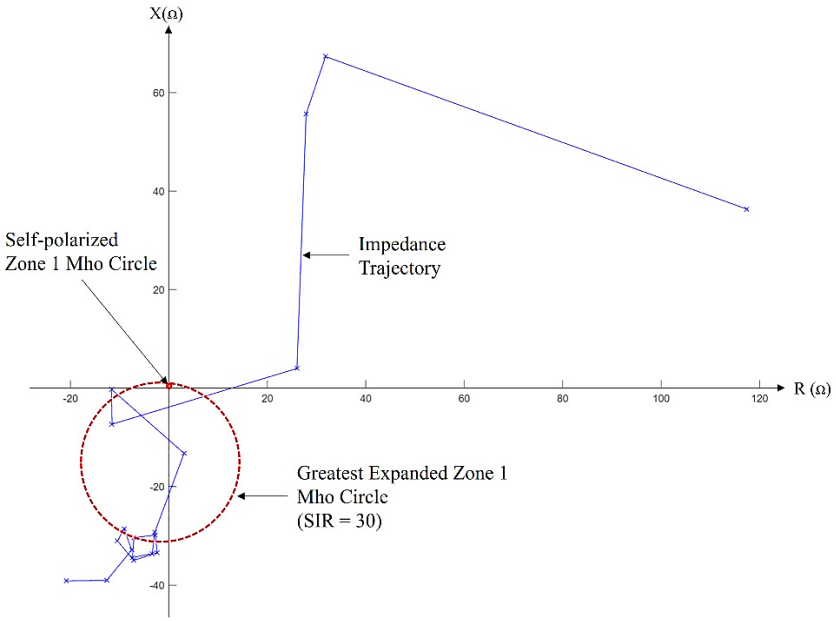

Fig. 9. ZAB Impedance trajectory seen by Relay 1 during the event

4.2. RELAY 2 & 4 ANALYSIS

Neither Relay 2 nor Relay 4 generated an event report during the event. Based on the event report settings, this means that the impedance trajectory seen from the Station C end never entered Zone 2 protection throughout the event.

4.3. RELAY 3 ANALYSIS

Since the source impedance ratio is the same at Relay 1 and Relay 3 and the lines have nearly identical construction parameters, the phase voltages and currents flowing on the lines were very similar. It would seem that if Relay 1 operated, Relay 3 should also have operated. After studying the settings of the two relays, it was discovered that the Zone 1 phase protection element on Relay 3 was disabled and therefore did not trip. It had been determined that the Zone 1 phase protection should be disabled on both relays due to high SIR. Relay 3 already had the setting disabled during a planned outage on Line C, while Relay 1 was awaiting a planned outage on Line B to make the change.

Fig. 10 shows the ZAB impedance trajectory with Zone 2 protection circle in Relay 3. The Zone 2 element was picked up at the start of the power swing, while the Mho circle was shrinking and before the time delay timed out, so the trajectory had already moved out of the circle.

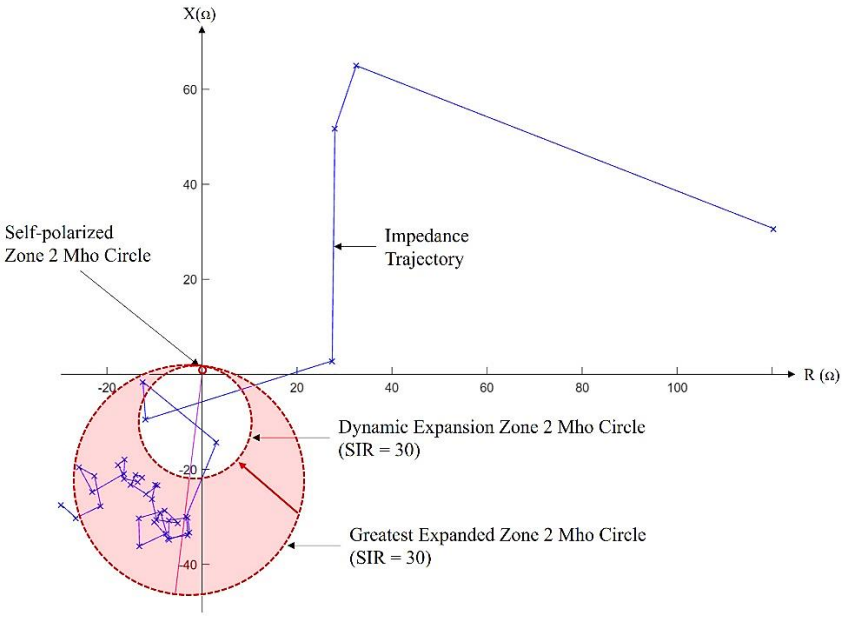

Fig. 10. ZAB Impedance trajectory seen by Relay 3 during the event

4.4. RELAY 5 ANALYSIS

A contributing factor to this event was the instantaneous reclosing of Station C terminal of Line F. The out-of-step logic for Relay 5 is configured to ensure that, when the relay identifies a power swing, instantaneous reclosing is blocked when the line terminal is tripped. Since the relay tripped due to a fault on Line F rather than on a power swing, instantaneous reclosing was not blocked during this event.

4.5. LINE A, B & C ANALYSIS

Three of the transmission lines experienced a short-duration overvoltage during the initial period of generator islanding. The most voltage-sensitive equipment in the islanded zone is the Coupling Capacitor Voltage Transformers, or CCVTs. All CCVT's are designed to handle short-term overvoltage conditions, but their capabilities vary by manufacturer. The data produced by a DFR at Station B indicated that the overvoltage had a peak magnitude of 167kV for 0.5 seconds. The CCVT's

installed have a rated voltage factor of 1.4/60s at a nominal primary voltage of 132.8kV. Thus, the overvoltage was not a cause for concern.

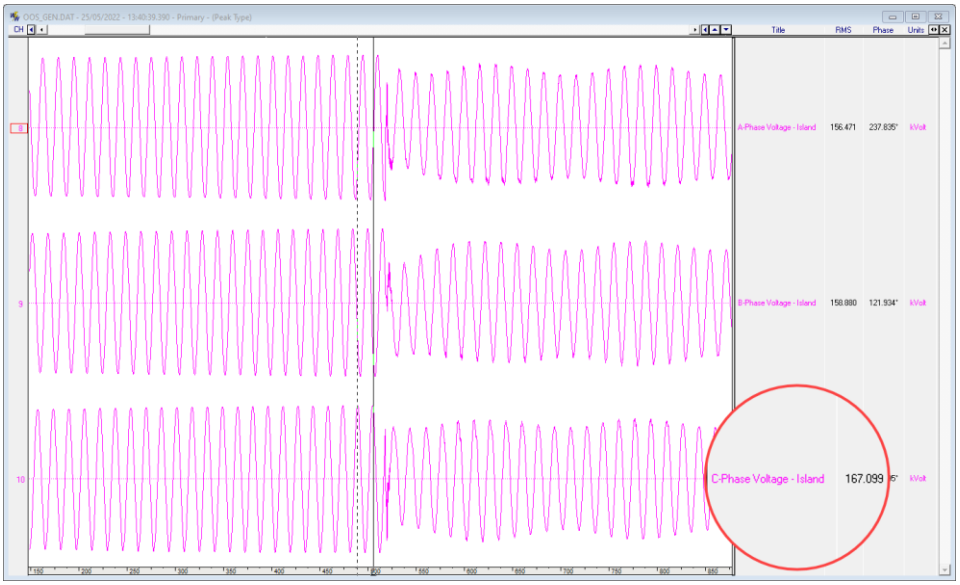

Fig. 11. Worst case overvoltage experienced on islanding side

5. ACTION TAKEN

To prevent further misoperation, automatic reclosing was disabled on Line F for the duration of the abnormal system configuration. Protection engineers reviewed the line protection to look for opportunities to prevent future misoperations. Since this event involved several lines in abnormal states, it was determined that further transmission protection setting changes would not increase reliability or prevent subsequent out-of-step operations.

The staff at the generation station was questioned about their response to the event. Plant operators reported that no damage was noted, but they did schedule an inspection for the next planned outage as a precaution.

6. CONCLUSION

This paper reviewed the theory and application of distance-based protection during a power swing near a hydro-generation facility. We scrutinized the relays in the area near the generator to determine why they did or did not operate. We introduced the concepts of self-polarization, cross-polarization, and positive-sequence-memory polarization and used them to validate that the voltages and currents observed during the power swing could have caused the relay events that occurred.

In the configuration, when the original network system is disconnected and becomes a radial feed, it is recommended to disable instantaneous reclosing at the first line that is radially connected to the grid. Although this may decrease the reliability of the system, it is preferable to avoid subjecting the generator or system to an oscillatory event.

BIBLIOGRAPHY

[1] D. D. Fentie, "Understanding the dynamic Mho distance characteristic," 2016 69th Annual Conference for Protective Relay Engineers (CPRE), College Station, TX, USA, 2016, pp. 1-15

[2] E. O. Schweitzer, III and J. Roberts, "Distance Relay Element Design," 19th Annual Western Protective Relay Conference, Spokane, WA, October 1992

[3] "IEEE Guide for Protective Relay Applications to Transmission Lines," in IEEE Std C37.113-2015 (Revision of IEEE Std C37.113-1999) , vol., no., pp.1-141, 30 June 2016

[4] [4]Nan Zhang and M. Kezunovic, "A study of synchronized sampling based fault location algorithm performance under power swing and out-of-step conditions," 2005 IEEE Russia Power Tech, St. Petersburg, Russia, 2005, pp. 1-7

[5] F. Calero, H. J. Altuve, "Identifying the Proper Impedance Plane and Fault Trajectories in Distance Protection Analysis," 38th Annual Western Protective Relay Conference, Spokane, WA, October 2011